

Magnetization switching in ferromagnetic microwiresA. Chizhik,¹ V. Zablotskii,^{2,3} A. Stupakiewicz,⁴ C. Gómez-Polo,² A. Maziewski,⁴ A. Zhukov,¹ J. Gonzalez,¹ and J. M. Blanco⁵¹*Departamento Física de Materiales, Facultad de Química, UPV, 1072, 20080 San Sebastián, Spain*²*Departamento de Física, Universidad Pública de Navarra, Campus de Arrosadía 31006 Pamplona, Spain*³*Institute of Physics, ASCR, CZ-182 21 Praha 8, Czech Republic*⁴*Laboratory of Magnetism, Faculty of Physics, University of Białystok, Lipowa 41, 15-424 Białystok, Poland*⁵*Departamento Física Aplicada I, EUPDS, UPV/EHU, Plaza Europa, 1, 20018 San Sebastián, Spain*

(Received 27 September 2010; published 1 December 2010)

Magnetization states of amorphous soft ferromagnetic microwires are studied by experiment and theoretically. It is shown that in low applied axial fields, on increasing the circular magnetic field produced by current, the initial homogeneous circular magnetization distribution evolves in three sequential steps: (i) the appearance of a helical magnetization state, (ii) a jump to the helical state with opposite chirality, and (iii) a gradual rotation of magnetization toward the new circular state. An applied, large-enough axial field stabilizes the axial magnetization states, making these transitions continuous and shifting the magnetic hysteresis loops. The origin of these successive magnetization reorientations and switching is explained in the frameworks of the proposed model.

DOI: [10.1103/PhysRevB.82.212401](https://doi.org/10.1103/PhysRevB.82.212401)

PACS number(s): 75.30.Gw, 75.50.Kj, 78.20.Ls

The physical properties of the ferromagnetic wires are being intensively studied in the latest decade. This is motivated by a need in deeper understanding of magnetism of low-dimensional systems¹ as well as by numerous possibilities of advanced technological applications.² With controlled anisotropy, the magnetization states can be tuned, and a stable micromagnetic configuration can be promoted in micron or submicron wires, which are needed for advanced sensors and biomedical applications.^{3,4} The importance of magnetic anisotropy is well recognized in tailoring micromagnetic configurations. Because of the interplay the shape (axial), radial and circumferential anisotropies, and amorphous ferromagnetic wires exhibit a rich variety of domain-line magnetic phases.^{2,5-8} These competing anisotropies originate in the distribution of internal stress which, depending on the thermal and/or mechanical prehistory of a wire, has axial, radial, and circumferential components.⁹ Thus, in a wire the actual distribution of stress-induced magnetic anisotropy is determined by the stress distribution as well as the sign and magnitude of magnetostriction. For example, for wires with negative magnetostriction axial anisotropy dominates in the inner core while circumferential anisotropy governs the magnetization in the outer shell.⁹ In such wires magnetization states represent either axially magnetized domains or circular and helical-like magnetization distributions.¹⁰⁻¹² The conception of a rigid inner core with a radius on the order of the domain-wall width, in which the magnetization is aligned parallel to the wire axis, has been successfully used to describe magnetization processes in relatively thick amorphous wires, 130 μm in diameter.¹³ On the contrary, thin ($\approx 20 \mu\text{m}$) nearly zero-magnetostrictive amorphous glass-coated microwires were recently well described with a model in which no core existence was assumed.¹⁰ On the other hand, any vortexlike magnetization state requires the existence of a nanometer-sized core (on the order of the exchange length) because of topological laws.¹⁴ Thus, when the wire diameter is pushed down to a submicron, e.g., see Ref. 5, both the magnetization states and the reversal are expected

to be affected by the actual inner core radius. As mentioned above, in a nearly zero-magnetostrictive amorphous glass-coated microwire the core radius is strongly dependent on the internal stress distribution.

In this Brief Report we present the result of current-induced transitions between different magnetic phases in ferromagnetic microwires. We suggest a phenomenological model, based on the assumption of a soft magnetic core, which allows us to describe the magnetization states and magnetization reversal of thin amorphous wires with negative, nearly zero magnetostriction. The model gives the four magnetization states of different chirality that are proven by the experiment. Moreover, our experiments and model demonstrate the existence of circularly and helically magnetized domains which are affected by the core radius. Note, with no radial magnetization component, the existence of circularly magnetized domains could not be explained by the contribution of magnetostatics. Investigation of the magnetization reversal process in microwires is one of the most important tasks related to the usage of such magnetic wires in different technological devices. In particular, intensive study of the magnetic properties of nearly zero magnetostriction Co-rich glass-covered microwires has been performed in relation with the giant magnetoimpedance effect. Moreover, ferromagnetic microwires can be used as model systems for the study of one-dimensional magnetic nanostructures. Consequently, the magneto-optical investigation of the magnetization reversal in the surface areas of microwires has become particularly important.

A glass-coated amorphous microwire with negative, nearly zero magnetostriction, of the nominal composition $\text{Co}_{67}\text{Fe}_{3.85}\text{Ni}_{1.45}\text{B}_{11.5}\text{Si}_{14.5}\text{Mo}_{1.7}$ [metallic nucleus radius $R = 11.2 \mu\text{m}$, glass coating thickness $\delta = 3 \mu\text{m}$, and a ratio of metallic nucleus diameter to total microwire diameter $\rho = 0.79$, see Fig. 1(a)] has been investigated by magneto-optical Kerr effect (MOKE) technique. The process of magnetization reversal in the surface area of the microwires has been studied by a MOKE loop tracer in transversal configu-

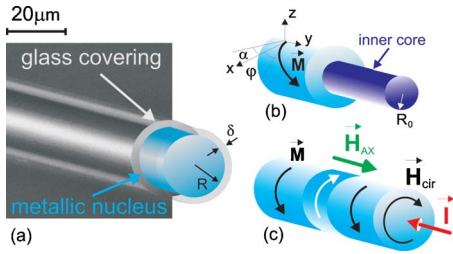


FIG. 1. (Color online) (a) Image and (b) schematic configurations of the wire with magnetization orientation, and (c) schematic of the circular domain nucleation and orientations of magnetic fields.

ration (T-MOKE) and by MOKE optical microscope in longitudinal configuration (L-MOKE) with the presence of a circular H_{cir} and axial magnetic field, H_{ax} [Fig. 1(b)]. To produce the circular magnetic field H_{cir} , an electric current I , flowing through the wire, was used. T-MOKE intensity of the reflected light is proportional to the magnetization M_x , which was perpendicular to the yz plane [Fig. 1(b)] of the light propagation.¹⁵ As a result of the MOKE magnetometry experiments, a series of Kerr intensity dependencies on the electric current I (the circular magnetic field) in the presence of dc bias H_{ax} has been obtained (see top panel in Fig. 2). Strong transformation of the hysteresis curves induced by H_{ax} has been found. The jump of the circular transversal magnetization becomes smoother and smaller with an axial magnetic field. Also the value of the normalized remanent magnetization M_r and the switching field H_{sw}^* (see Fig. 2), decrease with the increase in H_{ax} . The dc axial field produces a pronounced shift of the hysteresis loop along the horizontal axis. The direction of the shift depends on the sign of the axial field. When the axial magnetic field reached a certain value, the hysteresis was not observed and magnetization reversal took place as a coherent rotation of magnetization. The obtained results are sketched as the dependencies of the normalized M_r and H_{sw}^* (normalized to maximum value) on the dc axial field, and are presented in Figs. 2 and 4. These dependencies have a maximum value at about $H_{ax} = 0.27$ Oe.

The details and character of the circular magnetization reversal have been revealed using an L-MOKE microscope in Ref. 8. An experiment with increasing amplitude of the electric current (circular magnetic field) has been performed. The successive increase in the circular magnetic field induces the nucleation of the circular magnetic domains (the black area) in the surface of the microwire (inset, Fig. 4), followed by the propagation of domain walls along the microwire [a schematic of the circular domain nucleation is presented in Fig. 1(c)]. When $H_{ax} = 0$, the nucleation of two circular domains could be observed in the field of observation of the microscope at the first stage of magnetization reversal. Then, the relatively slow motion of the domain walls is finished by the collapse of the disadvantageous circular domain. In the presence of an axial magnetic field, the magnetization reversal is drastically changed. When the axial field reached the value of 0.27 Oe, the jump of circular magnetization was characterized by the nucleation of one domain and the long-distance quick motion of the solitary domain walls.

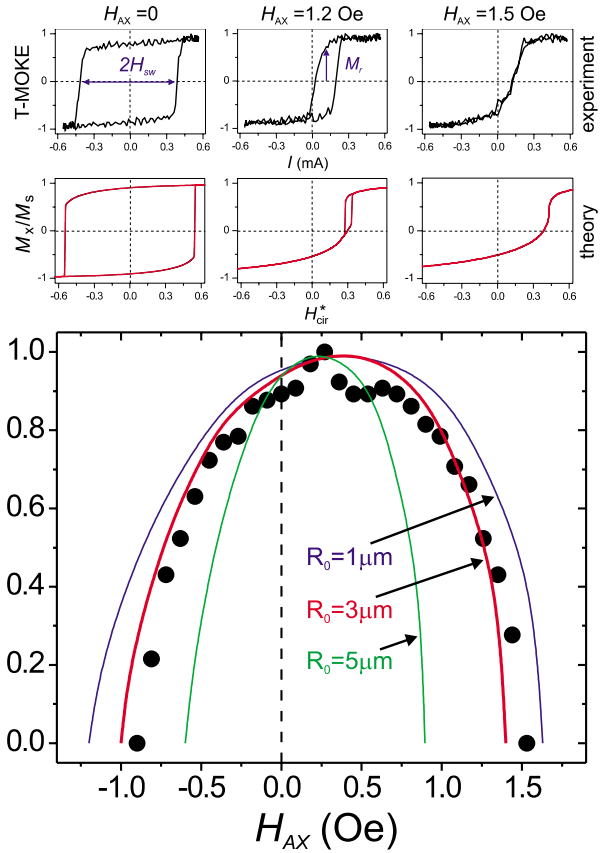


FIG. 2. (Color online) Top panel: the measured hysteresis loops and the loops— M_x/M_s vs H_{cir}^* —calculated from Eq. (1) for $H_{ax} = 0, 1.2,$ and 1.5 Oe. Dependence of normalized remanent circular magnetization component M_r on the external axial magnetic field H_{ax} (points). Lines are M_r calculated within the proposed model, assuming the anisotropy constants: $h_l = 2.9 \times 10^{-4}$, $h_a = 4.8 \times 10^{-4}$, and $\alpha = 20^\circ$ and the radius inner core $R_0 = 1, 3,$ and $5 \mu\text{m}$.

The obtained results can be interpreted in the framework of a phenomenological model which assumes the external circular and axial field-induced transformation of the surface magnetic structure. We consider that originally, under the zero axial magnetic field, the studied microwire has a helical magnetic structure in the surface area. Application of the axial magnetic field causes transformation of the surface magnetic structure and in particular, the change of the angle of the helicality (the direction of the circular magnetization in the surface area of the microwire). When the axial field is about 0.27 Oe the surface magnetization is directed strictly circularly. For this value of axial field, the surface magnetization reversal occurs as the jump between the two circular states and the jump of the circular magnetization has maximum value. The angle of the helicality could be controlled by the axial magnetic field H_{ax} . When the axial field is high enough, the magnetization with an axial direction is stable, which causes the disappearance of the circular hysteresis loop.

We assume that the magnetic structure of the studied microwire consists of a soft inner core with axial anisotropy and an outer shell in which the helical magnetic anisotropy dominates [Fig. 1(b)]. In other words, a wire consists of two

different areas—the core and shell—with different magnetic anisotropies: axial and helical, accordingly. The core radius is changeable, and depends on magnetic anisotropy distribution inside the wire. To determine the radius of the inner core we have performed fluxmetric experiments¹⁶ when the axial hysteresis loop is measured as a dependence of the axial magnetic field. Following,¹⁷ the value of the inner-core radius R_0 was determined to be about $3 \mu\text{m}$. Let us describe the magnetization states of a wire assuming that the magnetization vector has two components: circular and axial. The angle between the magnetization and the circular field (produced by the current) we denote as, see Fig. 1(b). As mentioned above, the inner core is assumed to have only axial magnetic anisotropy, and hereinafter we denote its radius as R_0 . The total energy of such a domain configuration is the sum of the anisotropy, Zeeman, and exchange energies

$$E(\varphi) = 2\pi^2 M_s^2 D [(R^2 - R_0^2) h_t \sin^2(\varphi + \alpha) + R_0^2 h_a \cos^2(\varphi + \alpha) - 2R^2 (h_{cir} \cos \varphi + h_{ax} \sin \varphi) + 2l_{ex}^2 \cos^2 \varphi \ln(R/l_{ex})], \quad (1)$$

where $l_{ex} = (A/2\pi M_s^2)^{1/2}$ is the exchange length, A is the exchange constant, and D is the domain length along the wire; is the angle between the helical anisotropy easy axis with the transversal direction [Fig. 1(b)], $h_a = H_{Aa}/4\pi M_s$ and $h_t = H_{At}/4\pi M_s$ are normalized axial and tangential (circular) anisotropy fields (where $H_{Aa} = 2K_a/M_s$ and $H_{At} = 2K_t/M_s$ are the anisotropy fields), $h_{cir} = H_{cir}/4\pi M_s$ is the scaled circular component of the applied field (due to current) and $h_{ax} = H_{ax}/4\pi M_s$. In Eq. (1), the last term represents the azimuthal exchange energy in the form derived in Ref. 18. Note, in Eq. (1) the magnetostatic energy contribution is zero because of the closed magnetic flux structure and we neglect the magnetic poles on the wire edges (a long wire). We now minimize Eq. (1) with respect to angle and calculate the magnetization hysteresis loops— M_x/M_s as a function of $H_{cir}^* = H_{cir}/H_{At}$ shown in Fig. 2 (top panel). Good agreement between the experimental and calculated magnetic hysteresis loops is seen from Fig. 2. In Fig. 2 for small applied axial fields $H_{ax} = 0$ and 1.2 Oe , the shown curves demonstrate the jumplike transitions between helical states of different chirality. On the circular field scale the jump points—the switching fields H_{sw} —are defined by two conditions: $\partial E/\partial \varphi = 0$ and $\partial^2 E/\partial \varphi^2 = 0$. The solution of these two equations gives us the switching circular field and critical angle of the magnetization φ_{cr} . In Fig. 3 we plot the critical angle as a function of the applied axial field for $\alpha = 0^\circ$ and 20° .

For each there are the four critical states corresponding to different chirality (left handed and right handed) and axial orientation (forward and backward) of the wire magnetization, see Fig. 3. The actual appearance of one of these four states depends on the magnetic prehistory of a wire. Upon changing H_{ax} the critical angle changes between 0 to π , and for $\alpha = 0$ when $H_{ax} = 0$ the shown states with $\varphi_{cr} = 0$ or $\varphi_{cr} = \pi$ correspond to the pure symmetrical circular magnetization states. For $\alpha \neq 0$ the magnetization states are asymmetrical and describe four helical magnetization states of different chirality (Fig. 3). Thus, in a low applied axial magnetic field,

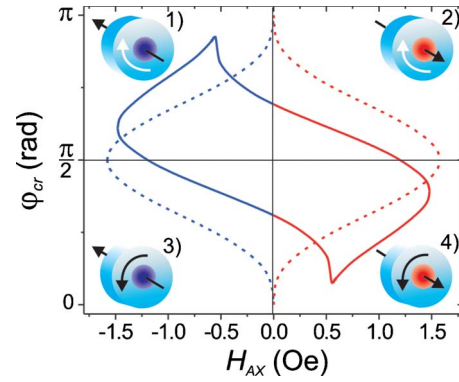


FIG. 3. (Color online) The critical angle φ_{cr} as functions of the axial applied magnetic field H_{ax} for $\alpha = 0^\circ$ (dashed line) and $\alpha = 20^\circ$ (solid line). Four magnetization states (1–4) corresponding to branches of $\varphi_{cr}(H_{ax})$, where the red and blue colors indicate the two directions of the axial magnetization (forward and backward).

a jumplike transition between helical states of different chirality takes place when the circular field (current) reaches the switching field value.

Equation (1) allows us to calculate, using the values of the magnetic anisotropy constants from,¹⁹ both the circular magnetization in the remanence state M_r and the normalized switching field H_{sw}^* as functions of the axial magnetic field for different radius inner core R_0 . These results are shown in Figs. 2 and 4, correspondingly. In Fig. 2 the calculated M_r are compared with the experimental data obtained for the wire with inner core radius $R_0 = 3 \mu\text{m}$ and $R = 11.2 \mu\text{m}$; there is good agreement between the experimental and calculated data. The $M_r(H_{ax})$ curves calculated for $R_0 = 1 \mu\text{m}$ and $R_0 = 5 \mu\text{m}$ predict the increase and decrease of the remanent magnetization, accordingly. In Fig. 4 we demonstrate the calculated and experimental curves: H_{sw}^* vs H_{ax} for the wire with three different core radiuses: $R_0 = 1, 3,$ and $5 \mu\text{m}$. Here the coincidence between the experimental and calculated curves is only satisfactory in the vicinities of the start-

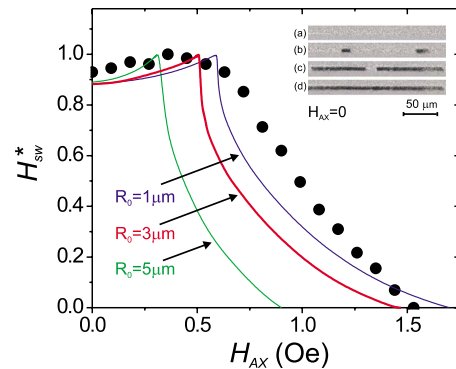


FIG. 4. (Color online) Switching field H_{sw}^* as a function of the applied axial magnetic field H_{ax} . The points are the measured while the lines represent the H_{sw}^* calculated from Eq. (1) for radius inner core $R_0 = 1, 3,$ and $5 \mu\text{m}$. The inset shows the magnetic domain structures without H_{ax} for different current: (a) 0; (b) 0.1 mA; (c) 0.4 mA; and (d) 0.8 mA. The wire was initially saturated (gray area) by the circular magnetic field $H_{cir} > 0$. The black areas are the magnetic domains induced by $H_{cir} < 0$ pulses.

ing and ending points of the field range change, $0 < H_{ax} < H_{ax0}$.

This discrepancy is explained by a domain structure which exists, namely, in this field range. Indeed, the magnetization states are barely circular or axial just at $H_{ax}=0$ and H_{ax0} so that they are monodomain states. In the moderate axial field, helical magnetic domains with different chirality appear, see the inset to Fig. 4. In order to switch the existing domain structure, an enhanced circular applied field is required because of an energy barrier related to the domain walls. Indeed, in a wire, magnetic domains of opposite chirality are separated by 180° domain walls. On increasing the current (circular field) the domains magnetized antiparallel to H_{cir} are squeezed and finally collapse. However, before the collapse the approaching domain walls could constitute 360° walls; namely, they lift the measured switching fields. This effect is similar to that known from physics of bubble materials: in low coercivity garnet films the existence of such domain walls leads to a significant increase of the saturation field—the field of the transition to the monodomain state.²⁰ A similar effect of the enhanced field stability of 360° domain walls has been theoretically proved for thin ferromagnetic films in Ref. 21. Note, in a wire with no radial anisotropy there is no magnetostatic reason for the domain appearance. In such wires the formation of irregular circularly magnetized domains is explained by heterogeneous nucleation processes that take place on applying a superposition of axial

and circular fields.⁸ These domains do not correspond to the energy minimum with respect to their period and therefore, such domains should be treated as metastable; this is a signature of magnetism of low-dimensional systems. Other examples of metastable domains can be found in Ref. 22.

To conclude, the magnetization states and magnetization switching in amorphous microwires were studied. In the studied wires the existence of four magnetization states with different chirality and axial direction is proven by experiment and theory. We propose a phenomenological model that describes magnetization states and their current-induced switching in wires with variable inner core radius. In low applied axial fields, on increasing the current (circular field), the initial left-handed chirality circular magnetization states undergoes the following phase sequence: a continuous transformation to a helical structure, then a jump to a helical state with opposite chirality, and finally, gradual rotation of the magnetization to a right-handed chirality circular state. An applied axial magnetic field smooths the jump between the states with opposite chiralities and makes the magnetization states asymmetrical. We have highlighted the role of the inner core in the formation of the magnetization states and magnetization reversal in such wires.

This work was supported by MICINN under Project No. MAT2007-66798.CO3.01 and Polish National Scientific Network SpinLab.

-
- ¹A. Masseboeuf, O. Fruchart, J. C. Toussaint, E. Kritsikis, L. Buda-Prejbeanu, F. Cheynis, P. Bayle-Guillemaud, and A. Marty, *Phys. Rev. Lett.* **104**, 127204 (2010).
- ²M. Vázquez and A. Hernando, *J. Phys. D: Appl. Phys.* **29**, 939 (1996).
- ³A. Hultgren, M. Tanase, C. S. Chen, G. J. Meyer, and D. H. Reich, *J. Appl. Phys.* **93**, 7554 (2003).
- ⁴D. S. Choi, J. Park, S. Kim, D. H. Gracias, M. K. Cho, Y. K. Kim, A. Fung, S. E. Lee, Y. Chen, S. Khanal, S. Baral, and J.-H. Kim, *J. Nanosci. Nanotechnol.* **8**, 2323 (2008).
- ⁵H. Chiriac, S. Corodeanu, M. Lostun, G. Ababei, and T.-A. Óvári, *J. Appl. Phys.* **107**, 09A301 (2010).
- ⁶M. Carara, K. D. Sossmeier, A. D. C. Viegas, J. Geshev, H. Chiriac, and R. L. Sommer, *J. Appl. Phys.* **98**, 033902 (2005).
- ⁷R. P. Erickson and D. L. Mills, *Phys. Rev. B* **80**, 214410 (2009).
- ⁸A. Chizhik, A. Stupakiewicz, A. Maziewski, A. Zhukov, J. Gonzalez, and J. M. Blanco, *Appl. Phys. Lett.* **97**, 012502 (2010).
- ⁹H. Chiriac and T.-A. Óvári, *J. Magn. Magn. Mater.* **249**, 141 (2002).
- ¹⁰M. Ipatov, V. Zhukova, A. Zhukov, J. Gonzalez, and A. Zvezdin, *Phys. Rev. B* **81**, 134421 (2010).
- ¹¹A. Chizhik, C. Garcia, A. Zhukov, J. Gonzalez, P. Gawronski, K. Kulakowski, and J. M. Blanco, *J. Appl. Phys.* **103**, 07E742 (2008).
- ¹²A. Chizhik, A. Zhukov, J. M. Blanco, J. Gonzalez, and P. Gawronski, *J. Magn. Magn. Mater.* **321**, 803 (2009).
- ¹³J. J. Freijo, A. Hernando, M. Vázquez, A. Méndez, and V. R. Ramanan, *Appl. Phys. Lett.* **74**, 1305 (1999).
- ¹⁴T. Shinjo, T. Okuno, R. Hassdorf, K. Shigeto, and T. Ono, *Science* **289**, 930 (2000).
- ¹⁵A. Chizhik, A. Zhukov, J. M. Blanco, and J. Gonzalez, *Phys. Status Solidi A* **189**, 625 (2002).
- ¹⁶A. Zhukov, M. Vázquez, J. Velázquez, H. Chiriac, and V. Larin, *J. Magn. Magn. Mater.* **151**, 132 (1995).
- ¹⁷A. M. Severino, C. Gómez-Polo, P. Marin, and M. Vázquez, *J. Magn. Magn. Mater.* **103**, 117 (1992).
- ¹⁸H. Hoffmann and F. Steinbauer, *J. Appl. Phys.* **92**, 5463 (2002).
- ¹⁹L. Kraus, M. Vázquez, G. Infante, G. Badini-Confaloneri, and J. Torrejón, *Appl. Phys. Lett.* **94**, 062505 (2009).
- ²⁰R. Gemperle, L. Murtinova, and J. Kaczer, *Acta Phys. Slov.* **35**, 216 (1985).
- ²¹C. B. Muratov and V. V. Osipov, *J. Appl. Phys.* **104**, 053908 (2008).
- ²²V. Zablotskii, W. Stefanowicz, and A. Maziewski, *J. Appl. Phys.* **101**, 113904 (2007).